Lab Invest 103 (2023) 100222

LABORATORY INVESTIGATION

journal homepage: https://laboratoryinvestigation.org/

Research Article

Identification of Proteomic Biomarkers in Proliferative Verrucous Leukoplakia through Liquid Chromatography With Tandem Mass Spectrometry

Esteban Arroyo[a], Mario Pérez Sayáns[b,c,*], Susana Belen Bravo[d], Camila de Oliveira Barbeiro[a], Mariana Paravani Palaçon[a], Cintia M. Chamorro Petronacci[d], María García Vence[d], María del Pilar Chantada Vázquez[d], Andrés Blanco Carrión[b], José M. Suárez Peñaranda[e], Abel García García[b], Pilar Gándara Vila[b,c], Janete Días Almeida[f], Giovani Carlo Veríssimo da Costa[g,h], Fábio César Sousa Nogueira[h], Joseph Albert Medeiros Evaristo[h], Denise de Abreu Pereira[i], Mirjami Rintala[j], Tuula Salo[k,l,m,n], Jaana Rautava[j,k,l], Elena Padín Iruegas[o], Monica G. Oliveira Alves[p], Túlio Morandin Ferrisse[q], Heitor Albergoni da Silveira[a], Jorge Esquiche León[r], Evânio Vilela Silva[a], Isadora Luana Flores[s], Andreia Bufalino[a]

[a] *Department of Diagnosis and Surgery, Araraquara, School of Dentistry, São Paulo State University (UNESP), Araraquara, São Paulo, Brazil;* [b] *Oral Medicine, Oral Surgery and Implantology Unit (MedOralRes), Faculty of Medicine and Dentistry, University of Santiago de Compostela, Instituto de los materiales de Santiago de Compostela (iMATUS), Santiago, Spain;* [c] *Instituto de Investigación Sanitaria de Santiago (IDIS) (ORALRES Group), Santiago de Compostela, Spain;* [d] *Proteomic Unit, Instituto de Investigación Sanitaria de Santiago (IDIS), Santiago de Compostela, Spain;* [e] *Servicio de Anatomia Patológica, Hospital Clinico Universitario de Santiago, Choupana s/n Santiago de Compostela, Spain;* [f] *Department of Bioscience and Buccal Diagnosis, São José dos Campos, Science and Technologies Institute, São Paulo State University (Unesp), São José dos Campos, São Paulo, Brazil;* [g] *Department of Basic Sciences, Nova Friburgo Health Institute, Univ. Federal Fluminense, Nova Friburgo, Rio de Janeiro, Brazil;* [h] *Laboratory of Proteomics, Technological Development Support Laboratory (LADETEC), Institute of Chemistry, Federal University of Rio de Janeiro, Rio de Janeiro, Brazil;* [i] *Program on Cellular and Molecular Oncobiology, Research Coordination, National Institute of Cancer (INCA), Rio de Janeiro, Brazil;* [j] *Department of Oral Pathology, University of Turku, Turku, Finland;* [k] *Department of Oral and Maxillofacial Diseases, Clinicum, University of Helsinki, Helsinki, Finland;* [l] *Department of Pathology, HUSLAB, Helsinki, Finland;* [m] *Department of Cancer and Translational Research Unit, University of Oulu, Oulu, Finland;* [n] *Medical Research Center Oulu, Oulu, Finland;* [o] *Human Anatomy and Embryology Area, Faculty of Physiotherapy, Department of Functional Biology and Health Sciences, Pontevedra, Spain;* [p] *Anhembi Morumbi University, School of Medicine, São José dos Campos, São Paulo, Brazil;* [q] *Department of Dental Materials and Prosthodontics, São Paulo State University (UNESP), School of Dentistry, Araraquara, Brazil;* [r] *Oral Pathology, Department of Stomatology, Public Oral Health, and Forensic Dentistry, Ribeirão Preto Dental School (FORP/USP), University of São Paulo, Ribeirão Preto, São Paulo, Brazil;* [s] *Oral Pathology Area, Conservative Dentistry Department, Dental School, Federal University of Rio Grande do Sul (UFRGS), Porto Alegre/RS, Brazil*

ARTICLE INFO

Article history:
Received 8 March 2023
Revised 13 July 2023
Accepted 19 July 2023
Available online 26 July 2023

Keywords:
calreticulin
leukoplakia
proliferative verrucous leukoplakia
proteomic

ABSTRACT

Proliferative verrucous leukoplakia (PVL) is an oral potentially malignant disorder associated with high risk of malignant transformation. Currently, there is no treatment available, and restrictive follow-up of patients is crucial for a better prognosis. Oral leukoplakia (OL) shares some clinical and microscopic features with PVL but exhibits different clinical manifestations and a lower rate of malignant transformation. This study aimed to investigate the proteomic profile of PVL in tissue and saliva samples to identify potential diagnostic biomarkers with therapeutic implications. Tissue and saliva samples obtained from patients with PVL were compared with those from patients with oral OL and controls. Label-free liquid chromatography with tandem mass spectrometry was employed, followed by qualitative and quantitative analyses, to identify differentially expressed proteins. Potential biomarkers were identified and further validated using immunohistochemistry. Staining intensity scan analyses were performed on tissue samples from patients

* Corresponding author.
E-mail address: mario.perez@usc.es (M. Pérez Sayáns).

https://doi.org/10.1016/j.labinv.2023.100222

with PVL, patients with OL, and controls from Brazil, Spain, and Finland. The study revealed differences in the immune system, cell cycle, DNA regulation, apoptosis pathways, and the whole proteome of PVL samples. In addition, liquid chromatography with tandem mass spectrometry analyses showed that calreticulin (CALR), receptor of activated protein C kinase 1 (RACK1), and 14-3-3 Tau-protein (YWHAQ) were highly expressed in PVL samples. Immunohistochemistry validation confirmed increased CARL expression in PVL compared with OL. Conversely, RACK1 and YWHA were highly expressed in oral potentially malignant disorder compared to the control group. Furthermore, significant differences in CALR and RACK1 expression were observed in the OL group when comparing samples with and without oral epithelial dysplasia, unlike the PVL. This research provides insights into the molecular mechanisms underlying these conditions and highlights potential targets for future diagnostic and therapeutic approaches.

Introduction

Oral potentially malignant disorders (OPMDs) are defined as any abnormality of the oral mucosa associated with a statistically increased risk of developing oral cancer.[1] The global prevalence rate of OPMD is approximately 5%, and predicting which lesions will progress to malignant tumors is a significant challenge.[2] Among OPMDs, oral leukoplakia (OL) and proliferative verrucous leukoplakia (PVL) share some clinical (irreversible white plaque) and microscopic (varying degrees of epithelial dysplasia) features but exhibit significantly different clinical manifestation and evolution.

OL has an incidence rate ranging from 1% to 4%, and a cumulative malignant transformation rate of 9.8%.[3] It primarily affects the vermilion of the lip, buccal mucosa, and gingiva and is more prevalent in men older than 40 years.[3] OL shares risk factors with oral squamous cell carcinoma (OSCC), such as tobacco use, excessive alcohol consumption, advanced age, chewing of areca nuts, and exposure to UV radiation when it affects the vermilion of the lip.[4]

In contrast, PVL presents clinically as a white plaque that becomes multifocal with aggressive, progressive, and irreversible manifestation.[1,5] The malignant transformation rate of PVL ranges from 14.3% to 75%, with an average rate of 49.5%.[6] Unlike OL, PVL does not appear to be associated with well-known risk factors for OSCC.[5] Moreover, the diagnosis and risk assessments of OPMD based on clinical and histopathological criteria suffer from poor reproducibility and high interobserver variability.[7-9] Recent evidence further highlights the lack of consensus in diagnosing PVL using this method.[10] Therefore, the early detection, prevention, and recognition of OSCC progression from PVL and OL lesions lack a standardized objective method. Additionally, PVL often exhibits an inadequate response to the existing treatment modalities, which fail to reduce relapses or the propensity for malignant transformation.[11] Consequently, a deeper understanding of the molecular nature of PVL is essential for developing new diagnostic and therapeutic tools.

The resolution of proteomics based on mass spectrometry (MS) has significantly improved because of recent developments and innovations, enabling more sensitive detection of proteins in tissues and saliva.[12-14] Different software packages allow differential quantitative analysis of the proteome, facilitating the exploration of clusters and nodes of different networks as well as their biological, functional, and metabolic pathways.[15-18] Consequently, identifying markers in tissues and saliva becomes essential for opening new possibilities in diagnosis and therapies. In this context, this study aimed to evaluate the significantly expressed proteins in tissues and saliva from PVL samples compared with those from OL and control/healthy individuals. We confirmed the overlapping proteins between oral tissues and saliva samples using proteomics based on MS. Additionally, we validated the selected biomarkers with therapeutic potential from this protein panel using immunohistochemical analysis. These biomarkers can serve as valuable resources for future studies related to PVL.

Materials and Methods

Patient Selection and Classification Criteria

The subjects of this study were divided into PVL, OL, and control groups. The classification of PVL and OL was based on a combination of previously defined clinical and histologic features of each disorder.[1] For the diagnosis of OL, the clinical aspects considered were the presence of a single plaque predominantly white in color, measuring <3 cm, that could not be rubbed off after excluding other clinically recognizable white or white/red lesions. The clinicopathological diagnosis of PVL was established for cases that clinically showed multiple white plaques ranging from flat to verrucous, spreading over time, with a total size of at least 3 cm when all affected areas were considered. In addition, all patients with OL and PVL included in this study had a minimum follow-up of 5 years after confirmation of the diagnosis. Histopathologically, tissue specimens from the OL and PVL exhibited features of hyperkeratosis with or without varying degrees of dysplasia (mild, moderate, or severe), following the new World Health Organization 2017 classification.[2] Additionally, samples were classified as "low-risk and "high-risk lesions" based on their potential susceptibility to malignant transformation, according to a previously proposed binary system.[7] Samples with verrucous hyperplasia, atypical verrucous hyperplasia, squamous cell carcinoma, or verrucous carcinoma were excluded. All tissue specimens were stained with hematoxylin and eosin and evaluated by 2 independent pathologists (E.V.S. and H.A.S.). In cases of disagreement between the examiners, a third tie-breaking examiner (J.E.L.) was consulted. Doubtful cases were immediately discarded and replaced. Inflammatory fibrous hyperplasia (IFH) was selected as the control because it is a reactive lesion that microscopically exhibits areas of chronic inflammation and has no risk of malignant transformation.

Sample Collection and Study Design

This study was conducted in 3 main steps, as illustrated in Figure 1. In step I, MS-based label-free quantitative analysis was conducted on the epithelial layer from laser-captured

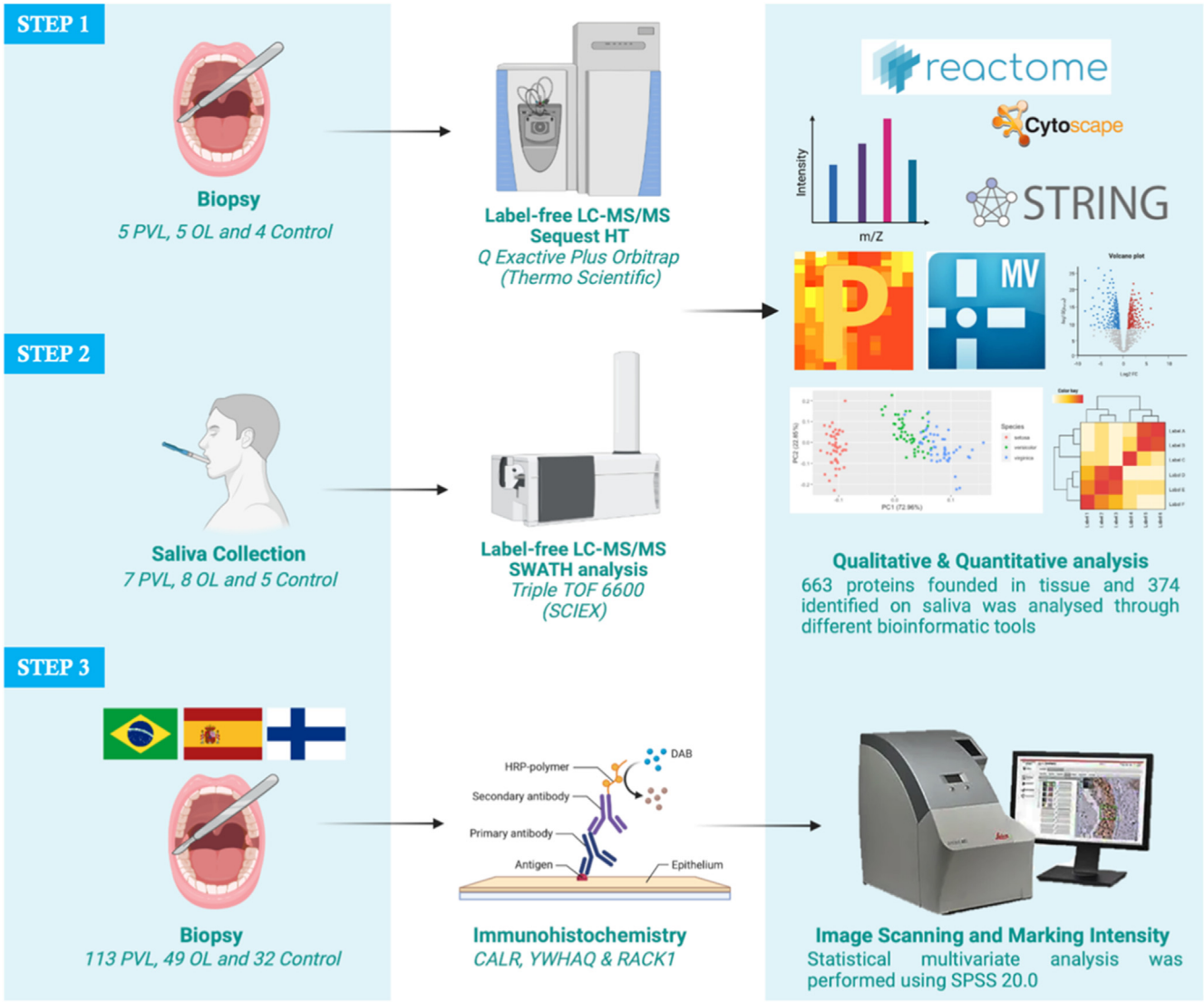

Figure 1.
Study design. This study comprised 3 main steps. Step I is the mass spectrometry–based label-free quantitative analysis conducted in the epithelial layer from laser capture microdissected frozen tissue samples obtained from patients with proliferative verrucous leukoplakia (PVL), oral leukoplakia (OL), and control group. Step II encompasses the label-free quantitative proteomic analysis using unstimulated saliva collected from the same groups. Finally, in step III, the differentially expressed proteins identified in the quantitative proteomic were validated using immunohistochemistry in paraffin-embedded specimens sourced from 3 countries. LC-MS/MS, liquid chromatography with tandem mass spectrometry; SWATH, Sequential Window Acquisition of all Theoretical Mass Spectra.

microdissected frozen tissue samples obtained from patients with PVL (n = 5), OL (n = 5), and IFH (n = 4). Differentially expressed proteins in the PVL were identified by comparing the proteomic profiles of the different groups. Step II involved label-free quantitative proteomic analysis using unstimulated saliva collected from patients diagnosed with PVL (n = 7), those diagnosed with OL (n = 8), and healthy individuals (n = 5). The clinical and pathological characteristics of the samples used in steps I and II are summarized in Supplementary Table S1. In step III, the differentially expressed proteins identified in the quantitative proteomic analysis were validated by immunohistochemistry (IHC) in other formalin-fixed paraffin-embedded samples. In total, 211 oral tissue samples were included in this study: 113 PVL samples, 49 OL samples, and 32 IFH samples as controls. Considering that PVL is a multifocal condition, the 113 PVL samples were obtained from 57 patients with PVL who underwent 2 biopsies, with samples collected from different oral sites during the period of follow-up. The clinical and pathological characteristics of the PVL and OL samples used in step III are summarized in Supplementary Table S2.

Laser Capture Microdissection, Protein Isolation, and Proteomics (Step I)

The frozen tissue samples were subjected to laser microdissection of the epithelial layer, aided by toluidine blue staining, using an Arcturus XT IR-Laser (Life Technologies). The microdissected samples were then coupled to caps, with 3 caps obtained for each sample. The caps were further coupled with tubes for protein extraction and digestion. The resulting peptides were transferred to an analytical column Poros R2 (Thermo Fisher) analog washed with trifluoroacetic acid 0.4%. After the protein digestion, normalization was performed considering the smallest

area of epithelium adhered to the cap, which corresponded to an area of 9,046,307 μm^2, resulting in a final volume of 20 μL.

Liquid chromatography coupled with tandem mass spectrometry (LC-MS/MS) was performed in triplicate using an Easy-nLC-1000 liquid chromatography system (Thermo Fisher) coupled to a Q Exactive Plus Orbitrap mass spectrometer (Thermo Fisher). The instrument operated in label-free data-dependent acquisition (DDA) mode with a dynamic exclusion of 45 milliseconds. Full-scan MS spectra were acquired at a resolution of 70,000, followed by fragmentation of the 15 most intense ions with collision cell CID and normalized collision energy of 30%, and a resolution of 17,500 in tandem mass spectrometry (MS/MS) scans. Unassigned species with a charge of +1 were excluded from MS/MS analysis.[19] Raw data were processed using Proteome Discoverer 2.1 Software (Thermo Fisher). Peptide identification was performed using the Sequest HT algorithm against the *Homo sapiens* database provided by UniProt. False discovery rates (FDR) were obtained using percolator node selection identification with a q value of $\leq$.01.

Protein levels were calculated on the basis of the area/spectrum intensity ratio obtained from Proteome Discoverer and loaded onto Perseus software version 1.6.10.43 (Max-Planck Institute of Biochemistry, Alemanha).[20] The data set underwent categorical annotation for each sample and group and subsequent filtration to retain rows based on a minimum of 70% valid values in at least 1 group of "samples." Venn diagram analysis as well as the analysis of biological interaction pathways and processes were performed using Reactome (http://www.reactome.org) and FunRich (http://www.funrich.org) open-access software, respectively.

Subsequently, the data were log2(×) transformed, and z-score normalized by column using the median. The median values of the technical replicates were calculated, followed by filtration of rows based on a minimum of 100% valid values in at least 1 group of "group."[15,19] Missing values for the label-free quantitation intensity were imputed with random numbers from a normal distribution, and their mean and SD were selected to simulate low-level values close to the noise level (imputation width, 0.3; shift, 1.8).

Multivariate statistical analysis using principal component analysis (PCA) was performed to compare data across samples (Benjamini–Hochberg FDR, 0.05). Volcano plots were constructed to explore the fold change values for protein expression in the PVL group compared with the OL and control groups (t test FDR, 0.05; S0, 0.1).[15,19] Proteins with a fold change greater than the threshold of 1.2 were categorized as exhibiting differential level.

Statistical analysis using 1-way analysis of variance (ANOVA), followed by Bonferroni post hoc test, was employed to determine significant differences in protein expression among the 3 groups (Permutation-based FDR, 0.05, with 250 randomizations). Enrichment theoretical analysis was performed to explore gene ontology of the biological process, cellular components, molecular function, and pathways using the Kyoto Encyclopedia of Genes and Genomes data from *H sapiens* annotations in the UniProt database.

To visualize the clustering and expression patterns of proteins in the samples, we constructed heat maps. Only proteins that exhibited differential expression values in the PVL group compared with the OL and control groups, as well as between the PVL and OL groups, and between the PVL and control groups, were selected for the heat maps. z-Score values of log2 label-free quantitation intensities were used for generating the heat maps. Contextual network analysis was conducted using Cytoscape through CHAT, considering the protein matrix of PVL vs OL fold change values (proteins with a fold change of >1.2).[17] Proteins with significant differential expression were further analyzed using the STRING open-access software (*H sapiens* database, confidence network edges, with the highest confidence value of 0.900, and hiding disconnected nodes) to create a network to highlight the clusters and nodes of interest.

Saliva, Protein Isolation, and Proteomics (Step II)

For Step II of this study, unstimulated saliva collection involved each subject swallowing and continuously expectorating into a sterile polypropylene conical tube for 5 to 10 minutes, resulting in a 5-mL saliva sample. To minimize the influence of food intake and circadian variation, all samples were collected at 8 to 9 AM after an overnight fasting state.[12] Two aliquots of 30 μL of saliva were precipitated using the method adapted from Dr Wessel's group. The resulting pellet was resuspended in Milli-Q water and subjected to in-gel concentration and digestion. To conduct global protein identification, an equal amount of protein (90 μg) from each sample was loaded onto a 10% SDS-PAGE gel. The protein bands were detected using Sypro-Ruby fluorescent staining (Lonza), excised, and subjected to in-gel manual tryptic digestion, as described previously.

For LC-MS/MS analyses, 4 μL (4 μg) of digested peptides were separated using an Ekspert nanoLC 400 liquid chromatography system coupled to a high-speed Triple TOF 6600 mass spectrometer (SCIEX) with a microflow source. The analytical column used was a silica-based reversed-phase column Chrom XP C18 150 × 0.30 mm with a 3 mm particle size and 120 Å pore size (SCIEX). The trap column was a YMC-TRIART C18 (YMC Technologies) with a 5 μm particle size and 120 Å pore size, which was switched online with the analytical column.

Data were acquired using the data-dependent workflow (DDA) approach. The equipment was operated using the Analyst TF 1.7.1 software (SCIEX). The ions selected for MS/MS analysis had a mass-to-charge ratio (m/z) greater than 350 and smaller than 1400 m/z, with a charge state of 2 to 5. The mass tolerance was set at 250 ppm, and the level threshold to more than 200 counts (cps). The instrument was automatically calibrated every 4 hours using external standard tryptic peptides obtained from PepCalMix solution. After MS/MS analysis, data files were processed using the ProteinPilotTM 5.0.1 software (SCIEX). A search was performed against the Human-Specific UniProt database, and a nonlinear fitting method was used for FDR calculation. Only results reporting 1% global FDR or better were considered. To ensure the representation of peptides and proteins in all the samples, pooled vials of samples from each group were prepared using equal mixtures of the original samples.

The MS/MS spectra of the identified peptides were then used to generate a spectral library for Sequential Window Acquisition of all Theoretical Mass Spectra (SWATH), performed using PeakView (version 2.2) with the SWATH Acquisition MicroApp (version 2.0). PeakView computed the FDR and the score for each assigned peptide based on the chromatographic and spectral components, with only peptides with an FDR of 1% used for protein quantitation.

The integrated peak areas were exported to MarkerView software (SCIEX) for relative quantitative analysis. Unsupervised multivariate statistical analysis using PCA was performed to compare the data across the samples. The PCA plots were generated using the square root and range-scale parameters. The average MS peak area of each protein was calculated from the replicates, and the Student t test was used to compare the samples on the basis of the averaged area sums of all transitions derived for each protein. The t test indicates how well each variable distinguishes the 2 groups, reported as a P value.

A general overview of exclusive and common proteins among the groups was obtained using the library of the Protein Pilot database selecting proteins with an FDR of <1% and using a Venn diagram (Bioinformatics & Evolutionary Genomics software). Biological interaction pathways and processes were analyzed using Reactome[16] and FunRich[21,22] open-access software (Functional Enrichment Analysis Tool), respectively. For this library, proteins were considered differentially expressed with a q value of <.05 and a fold change of >1.2 or <0.83.

Furthermore, all proteins identified in the PVL saliva samples, as well as proteins showing differential expression, were separately loaded into the STRING open-access software (using *H sapiens* database, confidence network edges, with the highest confidence value = 0.900, and hiding disconnected nodes) to create 2 different networks highlighting the clusters and nodes formed by these proteins.

Immunohistochemistry (Step III)

Paraffin sections were dewaxed in xylene and rehydrated in a series of graded alcohol solutions (95%, 80%, and 70%). IHC for cell typing was conducted using primary antibodies against calreticulin (CALR, FMC 75; Abcam; 1:2.000), 14-3-3 Tau-protein (YWHAQ, A2563; ABclonal; 1:200), and receptor of activated protein C kinase 1 (RACK1, A0151; ABclonal; 1:200). The sections were then incubated with a solution containing 0.6 mg/mL 3,3′diaminobenzidine tetrahydrochloride (Sigma) and counterstained with Harris hematoxylin. Negative controls were included in all reactions by suppression of primary antibodies.

For quantification, high-resolution images of the glass slides were scanned and analyzed using the Pixel Count V9 algorithm software (Aperio ImageScope 12.4.3, Leica Biosystems). The epithelial area was delineated, and specific input parameters were used for each antibody (hue value, hue width, and color saturation threshold) to calculate the percentage of cytoplasmic positivity. The staining intensity was categorized into 3 ranges: weak, moderate, and strong. Intensity scores were assigned as follows: 1 = weak, 2 = moderate, and 3 = strong. The final marking intensity scores were calculated as the sum of the percentages of each category weighted by its intensity score using the following equation: $[(\%\text{weak} \times 1) + (\%\text{moderate} \times 2) + (\%\text{strong} \times 3)]$.

Statistical analysis was conducted by an independent statistician who remained blinded to the group comparisons. Normal distribution was assessed using asymmetry and kurtosis analyses, and outliers were evaluated. Homoscedasticity was assessed using Box's Test of Equality of Covariance Matrices and Levene's test for the equality of variances. Therefore, a multivariate 1-way ANOVA was conducted. Additionally, a 2-way ANOVA was applied to evaluate the association of CALR, YWHAQ, and RACK1 with the presence and absence of tissue dysplasia in OL and PVL. Differences between groups were analyzed using the Games–Howell post hoc test. Statistical analysis was performed using IBM SPSS Statistics 20.0 ($\alpha = 0.05$), and graphics images were generated using GraphPad Prism version 6.0.

Results

Biomarker Discovery and Candidate Selection on the PVL Tissue

A total of 663 proteins were identified from Proteome Discoverer (FDR, ≤0.01) in the tissue samples across the 3 groups. After applying the filtering criteria as described in the previous section, 309 proteins were retained. Venn diagram analysis revealed that 120 proteins were identified simultaneously in the 3 groups, whereas 110 were exclusively expressed in the PVL group (Fig. 2A and Supplementary Table S3). The number of proteins detected exclusively in the PVL group was significantly higher than that of the OL and control groups. Using the UniProt code for each protein in the PVL group, 266 out of 305 identifiers were found in the Reactome, resulting in the identification of 851 pathways affected by at least 1 of these proteins. The most significantly represented pathways were related to the immune system, cell cycle, DNA replication, apoptosis, and protein metabolism (Supplementary Table S4). In the OL group, 137 of 157 identifiers in the sample were found in the Reactome, revealing 652 pathways affected by at least one of these proteins. The most significantly represented pathways in this group were related to DNA repair, apoptosis, cellular responses to stress, the immune system, and the cell cycle (Supplementary Table S5).

Furthermore, the FunRich analysis tool showed that compared with the OL group, most proteins identified in the PVL were associated with biological processes related to inflammatory pathways (tumor necrosis factor–mediated signaling pathway and antigen processing and presentation via MHC class I), the MAPK cascade, and Wnt signaling pathways (Supplementary Fig. S1A).

The data set of the 309 proteins matrix was further processed and filtered, resulting in a new matrix containing 89 proteins. PCA with these 89 proteins demonstrates that PVL tissue samples are well separated from OL and control samples by protein expression profiles (Fig. 2B).

Differential protein concentration analysis using a ±1.2-fold change cutoff and FDR ≤ 0.05 revealed 32 significantly upregulated proteins in PVL compared with OL tissue samples, as well as 35 significantly upregulated and 2 significantly downregulated proteins in PVL compared with IFH samples (Fig. 2C, D). A Bonferroni post hoc test identified 51 proteins with significant differences in levels among the 3 groups. After theoretical analysis of the enrichment of these proteins, only 48 proteins showed statistically significant differences in expression among the 3 groups (Table 1). Among these, 18 proteins were differentially expressed in the PVL group compared with the OL and control groups, 11 proteins were differentially expressed between the PVL and OL groups, and 14 proteins were differentially expressed between the PVL and control groups. Moreover, 5 proteins (KRT4, KRT78, KRT1, KRT10, and UBA1) exhibited statistical differences in the main test; however, the post hoc test could not identify the groups in which these differences occurred. This discrepancy between the main test and post hoc results is likely related to the similarities between the OL and control groups, which were nearly identical in most cases. Heat map analysis revealed significant differences in protein expression between the PVL tissue samples and the OL and control samples, with the PVL samples forming a distinct cluster (Fig. 2E).

The Cytoscape analysis revealed that the YWHA family proteins exhibited the highest level of interaction with other proteins (Fig. 2F). Additionally, the STRING network analysis, based on the same sample matrix, revealed 6 distinct clusters (Fig. 2G). Among these clusters, YWHA family proteins were connected to 2 other clusters composed of heat shock proteins, including CALR, ALDOA, GAPDH, GDI2, and RAB11A. Two other clusters were associated with the ribosomal protein RACK1 and keratin-associated proteins.

To select potential biomarkers, 4 criteria were considered: (1) significant differential expression proteins (1.2-fold change cutoff and an FDR of 0.05) between PVL against OL and control groups;

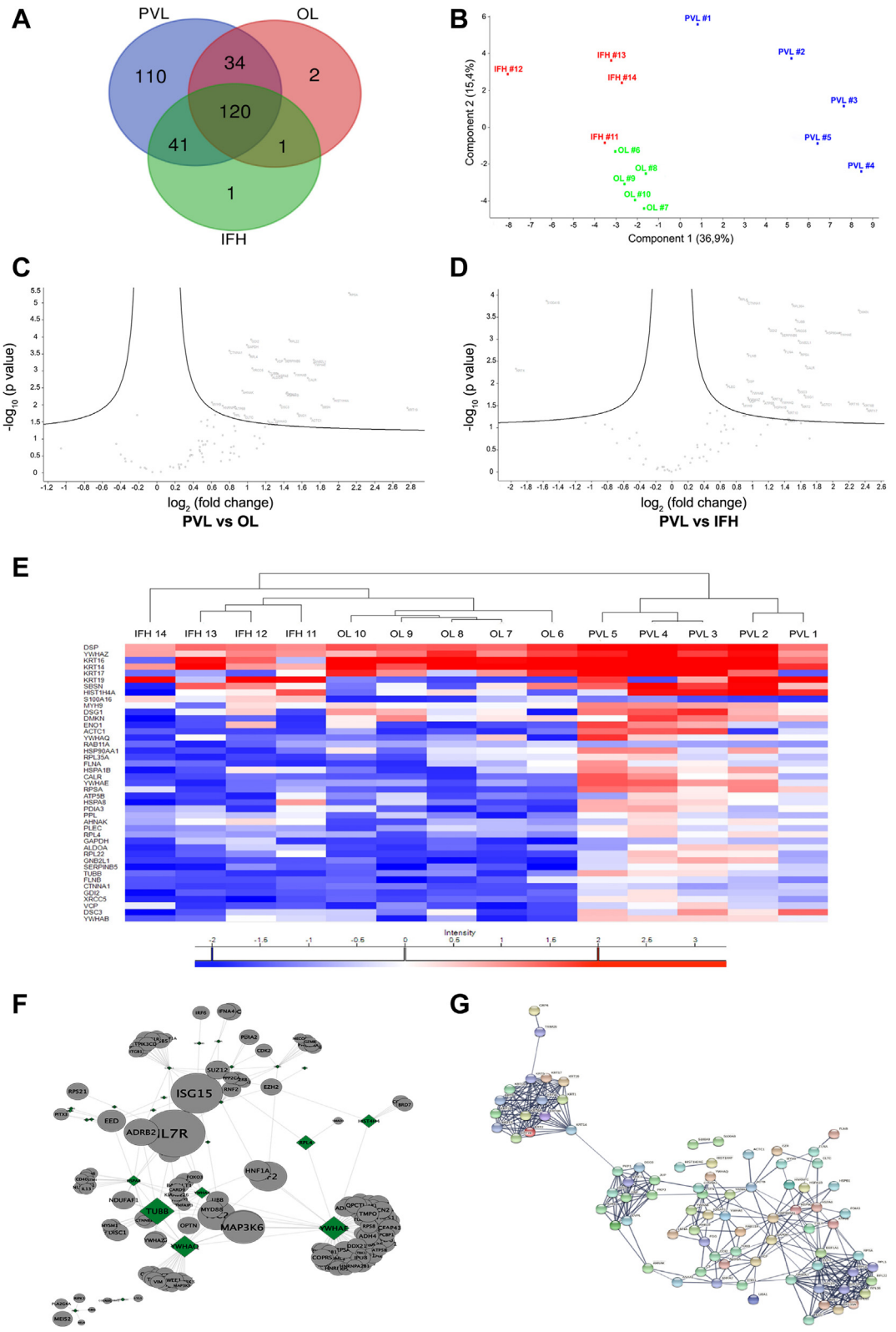

Figure 2.

Analysis of protein quantity in tissue samples from the proliferative verrucous leukoplakia (PVL), oral leukoplakia (OL), and control (inflammatory fibrous hyperplasia [IFH]) groups. (A) Venn diagram analysis illustrating the proteins in tissue samples from PVL, OL, and control groups. (B) PC1 separated PVL samples (right side of the graph) from the rest of the OL and IFH groups (closer to each other on the left side). (C, D) Volcano plots analysis comparing protein expressions in the PVL and OL and control groups. A threshold of ±1.2 for up/down expression was applied. (D) Results of heat map analysis of differentially expressed proteins of PVL, OL, and control (upregulation depicted in red and downregulation in blue). (E) Contextual network analysis using CHAT on Cytoscape, presenting the 43 differentially expressed proteins with fold change values > 1.2, highlighted in green. (F) A functional network of 43 differentially expressed proteins visualized using STRING, with each colored ball representing a protein and the thickness of the connecting line indicating the functional relationship between the proteins.

Table 1
Statistically significant differential expression of proteins identified in proteomic analysis of proliferative verrucous leukoplakia compared with oral leukoplakia and control tissues (inflammatory fibrous hyperplasia)

Protein name	Gene symbol	FC PVL vs OL	FC PVL vs Ctrl	DE *q* value
40S Ribosomal protein SA	*RPSA*[a]	2.1	1.6	<.001
Histone H4	*HIST1H4A*[b]	1.9	1.6	.02
14-3-3 protein epsilon	*YWHAE*[a]	1.7	2.1	<.001
Alpha-enolase	*ENO1*[b]	1.6	1.4	.03
14-3-3 protein beta/alpha	*YWHAB*[a]	1.5	1.0	.01
Serpin B5	*SERPINB5*[a]	1.4	1.4	<.001
Heat shock 70 kDa protein 1B	*HSPA1B*[b]	1.4	1.3	.02
14-3-3 protein theta	*YWHAQ*[a]	1.3	1.4	.02
Fructose-bisphosphate aldolase A	*ALDOA*[b]	1.3	0.9	.01
Heat shock cognate 71 kDa protein	*HSPA8*[b]	1.3	1.3	.03
Desmoglein-1	*DSG1*[c]	1.1	1.6	.04
Keratin, type II cytoskeletal 1	*KRT1*[c]	1.1	1.5	.04
Rab GDP dissociation inhibitor beta	*GDI2*[a]	1.0	1.2	<.001
Glyceraldehyde-3-phosphate dehydrogenase	*GAPDH*[b]	1.0	0.4	.01
ATP synthase subunit beta, mitochondrial	*ATP5B*[c]	0.9	1.1	.02
Keratin, type I cytoskeletal 10	*KRT10*[c]	0.8	1.4	.04
14-3-3 protein zeta/delta	*YWHAZ*[c]	0.5	0.9	.03
Keratin, type I cytoskeletal 16	*KRT16*[c]	0.3	2.2	.01
Keratin, type I cytoskeletal 14	*KRT14*[c]	0.1	1.2	.02
Keratin, type II cytoskeletal 4	*KRT4*[c]	−1.1	−1.9	.04
Keratin, type I cytoskeletal 19	*KRT19*[b]	2.8	−0.2	.01
Suprabasin	*SBSN*[b]	1.8	1.4	.03
Receptor of activated protein C kinase 1	*GNB2L1*[a]	1.7	1.6	<.001
Calreticulin	*CALR*[a]	1.7	1.7	<.001
Actin, alpha cardiac muscle 1	*ACTC1*[a]	1.7	1.9	.01
60S ribosomal protein L22	*RPL22*[a]	1.5	0.9	<.001
Protein disulfide-isomerase A3	*PDIA3*[b]	1.4	0.9	.01
Desmocollin-3	*DSC3*[a]	1.4	1.6	.01
Transitional endoplasmic reticulum ATPase	*VCP*[a]	1.3	1.0	.01
Tubulin beta chain	*TUBB*[b]	1.2	1.5	<.001
Keratin, type II cytoskeletal 78	*KRT78*[b]	1.2	0.1	.04
X-ray repair cross-complementing protein 5	*XRCC5*[a]	1.1	1.5	<.001
60S ribosomal protein L4	*RPL4*[a]	1.0	0.8	<.001
Neuroblast differentiation-associated protein AHNAK	*AHNAK*[b]	0.9	1.1	.01
Filamin-B	*FLNB*[a]	0.9	0.9	.02
Filamin-A	*FLNA*[c]	0.9	1.4	.01
Periplakin	*PPL*[b]	0.9	0.2	.02
Catenin alpha-1	*CTNNA1*[a]	0.8	0.9	<.001
Keratin, type I cytoskeletal 17	*KRT17*[c]	0.7	2.4	.03
Heat shock protein HSP 90-alpha	*HSP90AA1*[c]	0.7	1.9	<.001
Myosin-9	*MYH9*[c]	0.6	1.7	.02
60S ribosomal protein L35a	*RPL35A*[c]	0.6	1.5	<.001
Plectin	*PLEC*[a]	0.6	0.7	.02
Desmoplakin	*DSP*[c]	0.6	0.9	.01
Ubiquitin-like modifier-activating enzyme 1	*UBA1*[b]	0.5	0.4	.04
Dermokine	*DMKN*[c]	0.5	2.3	<.001
Protein S100-A16	*S100A16*[c]	−0.1	−1.6	<.001
Ras-related protein Rab-11A	*RAB11A*[c]	−0.2	0.5	.01

Fold change threshold was ±1.2. Differential expression considered a false discovery rate of 0.05. Inflammatory fibrous hyperplasia was considered as control.
Ctrl, control; DE, differential expression; FC, fold change; OL, oral leukoplakia; PVL, proliferative verrucous leukoplakia.
[a] Proteins that show the difference between proliferative verrucous leukoplakia against oral leukoplakia and control groups at the same time.
[b] Proteins that only show the difference between proliferative verrucous leukoplakia and oral leukoplakia groups.
[c] Proteins that only show the difference between proliferative verrucous leukoplakia and control groups.

(2) proteins with gene ontology annotations related to the cell cycle, immune system, DNA repair, and programmed cell death; (3) theoretical analysis–based identified proteins involved in malignant transformation and with therapeutic potential; and (4) proteins with the highest level of interaction with one another, as this could provide insights into synergistic effects of altered expression. Based on these criteria, 3 candidate biomarkers were selected for further validation, namely CALR, YWHAQ, and RACK1.

Proteome Overview of Saliva and Proteins Simultaneously Identified in the PVL Tissue and Saliva Samples

A total of 374 proteins (FDR, ≤ 0.01) were identified using ProteinPilot across the 3 groups. Specifically, 282 corresponded to the PVL, 287 to the OL, and 247 to the control group. The Venn diagram revealed that 190 proteins were common to the 3 groups, with 53 and 49 proteins unique to

PVL and OL, respectively (Fig. 3A and Supplementary Table S6).

Using the uniport code of each protein in the PVL group, 285 of the 369 identifiers in the sample were found in the Reactome database, of which 1034 pathways were hit by at least one. The most significantly represented pathways were related to the immune system and apoptosis (Supplementary Table S7). In the OL group, 231 of the 287 identifiers in the sample were found in the Reactome, with 908 pathways being hit by at least one of these proteins. The most significantly represented pathways were related to the immune system, DNA repair, and cell cycle (Supplementary Table S8). In addition, the saliva analysis indicated that the PVL group had a higher number of proteins linked to biological processes involving the immune system, cell cycle control, programmed cell death, cell activity, and phenotypic characteristics compared with the OL group (Supplementary Fig. S1B). PCA results obtained from the saliva samples demonstrated only a subtle differentiation of the samples into 3 groups based on the protein expression profiles (Fig. 3B).

Differentially expressed proteins based on an FDR of <0.05 and fold change threshold of ±1.2 revealed 51 proteins with statistically significant differences in level among the 3 groups (Table 2). Among these proteins, 21 were differentially expressed in the PVL group compared with the OL and control groups, 7 were differentially expressed between the PVL and OL groups, and 23 were differentially expressed between the PVL and control groups. The majority of the identified proteins were downregulated in PVL saliva samples compared with OL and control saliva samples.

Furthermore, we examined the number of proteins identified simultaneously in PVL tissue and saliva samples. We identified 67 proteins simultaneously in the PVL tissue and saliva samples, whereas 238 and 215 proteins were identified exclusively in the PVL tissue and saliva, respectively (Fig. 3C). Of the 48 differentially expressed proteins in the tissues among the 3 groups, 20 overlapping proteins were observed in both tissue and saliva samples (Table 3). Among these, only 4 proteins (Serpin B5, GAPDH, keratin 14, and desmoglein-1) exhibited differential expression in the saliva based on the FDR and fold change threshold. Candidate biomarkers CALR and RACK1, which were selected in the tissue for validation, were not identified in the saliva proteome. However, YWHAQ was identified in the saliva proteome but did not show differential expression in the saliva of the PVL group compared with the other 2 groups.

Validation of Potential Biomarkers by Immunohistochemical Staining

To validate the results for the t3 selected potential biomarkers, immunohistochemical staining was performed for CALR, YWHAQ, and RACK1 in archived tissue samples from PVL, OL, and IFH. Immunohistochemical staining for all biomarkers revealed a cytoplasmic staining pattern in epithelial cells in all groups but showed differences in staining intensity between PVL, OL, and IFH. Nuclear positivity was observed in some samples for YWHAQ and RACK1. In addition, discrete immunohistochemical staining was observed for all markers in stromal cells, including inflammatory cells, spindle-shaped mesenchymal cells, and endothelial cells.

To assess statistical differences in staining intensity, clinicopathological diagnoses of PVL, OL, and IFH were considered as independent variables, whereas the intensity of immunohistochemical staining for CALR, YWHAQ, and RACK1 served as

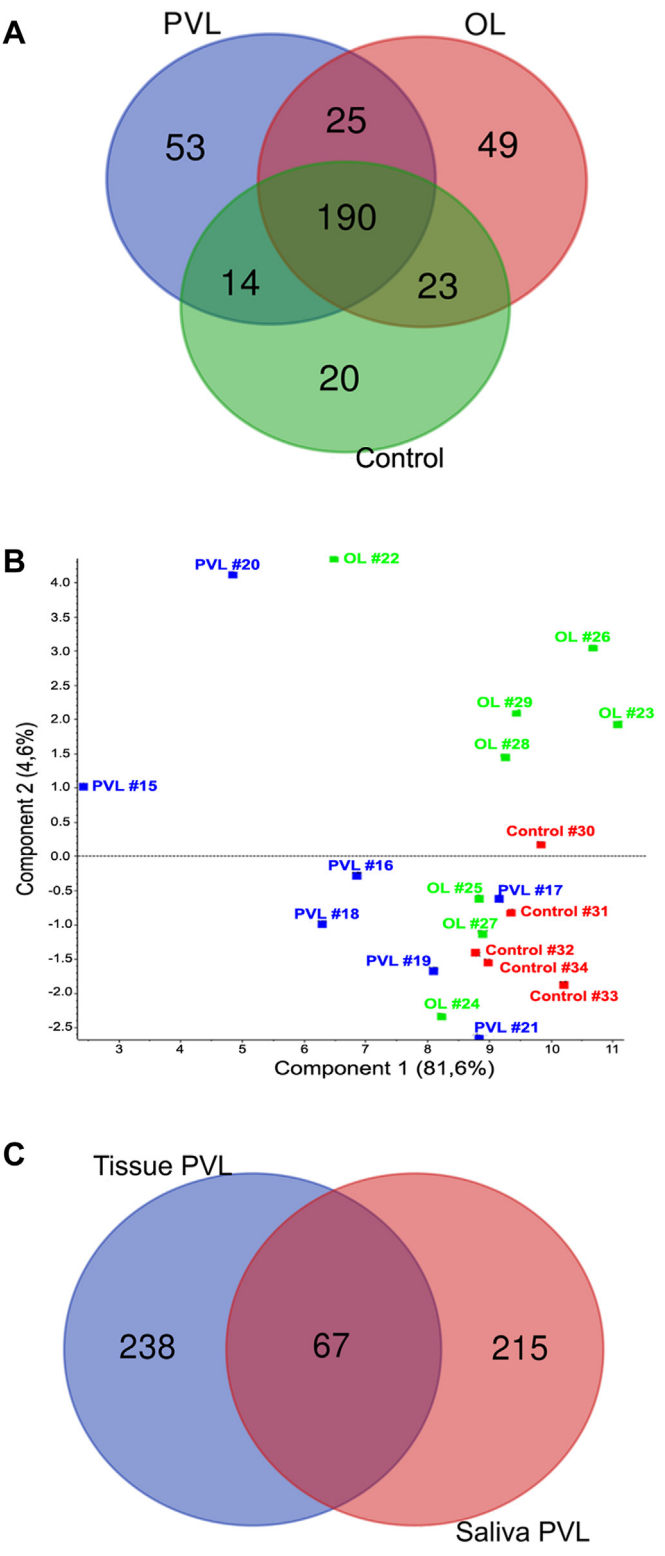

Figure 3.
Analysis of protein quantity in saliva samples from the proliferative verrucous leukoplakia (PVL), oral leukoplakia (OL), and control groups. (A) Venn diagram illustrating the overlap of 67 proteins identified in tissue and saliva samples from the PVL. (B) PC1 separated most PVL saliva samples (left side of the graph) from the OL (center of the graph) and control (right side of the graph) groups. (C) Venn diagram analysis of the proteins simultaneously identified in the PVL tissue and saliva samples.

Table 2
Statistically significant differential expression of proteins identified in proteomic analysis of saliva from proliferative verrucous leukoplakia compared with oral leukoplakia and healthy individuals

Protein name	Gene symbol	FC PVL vs OL	FC PVL vs Ctrl	DE *q* value
Adenosylhomocysteinase	*AHCY*[a]	−0.99	−1.84	.002
Beta-2-microglobulin	*B2M*[b]	−1.68	−1.41	.002
BPI fold−containing family B member 2	*BPIFB2*[b]	−1.85	−1.71	.01
Carboxypeptidase E	*CPE*[b]	−2.14	−1.76	.007
Cell division control protein 42 homolog	*CDC42*[b]	−1.34	−2.11	.001
Chloride intracellular channel protein 1	*CLIC1*[b]	−1.21	−2.19	.001
Cocaine esterase	*CES2*[b]	−1.32	−1.72	<.001
Desmoglein-1	*DSG1*[a]	−1.03	−1.75	.002
ERO1-like protein alpha	*ERO1A*[b]	−1.54	−1.85	<.001
Heme-binding protein 2	*HEBP2*[b]	−2.11	−1.80	<.001
IgGFc-binding protein	*FCGBP*[b]	−2.35	−1.77	.03
Interleukin-1 receptor antagonist protein	*IL1RN*[b]	−1.45	−1.40	.001
Interleukin-36 alpha	*IL36A*[b]	−2.02	−2.54	<.001
Kallikrein-11	*KLK11*[c]	−1.55	−1.13	.04
Keratin, type I cytoskeletal 13	*KRT13*[c]	−1.64	−1.10	.01
Keratin, type I cytoskeletal 14	*KRT14*[b]	−1.3	−1.77	.02
Liver carboxylesterase 1	*CES1*[b]	−1.72	−2.03	.01
Ly6/PLAUR domain-containing protein 3	*LYPD3*[b]	−1.97	−2.47	.008
Mesothelin	*MSLN*[b]	−2.48	−3.17	.01
Mucin-5B	*MUC5B*[a]	−2.09	−2.33	.04
Nucleobindin-1	*NUCB1*[b]	−3.28	−1.67	.01
Nucleotide exchange factor SIL1	*SIL1*[b]	−1.82	−1.27	.01
Prostaglandin reductase 1	*PTGR1*[b]	−1.26	−1.64	.001
Proteasome activator complex subunit 2	*PSME2*[b]	−1.75	−2.27	<.001
Putative cytochrome P450 2D7	*CYP2D7*[a]	−2.85	−2.99	.04
Ras-related protein Rap-1A	*RAP1A*[b]	−1.36	−1.59	.003
Transforming protein RhoA	*RHOA*[a]	−0.36	−2.23	.04
Transgelin-2	*TAGLN2*[b]	−1.41	−1.48	.001
Cystatin-S	*CST4*[c]	−1.92	−1.74	.04
Cysteine-rich secretory protein 3	*CRISP3*[c]	−1.39	−0.69	.02
Nucleobindin-2	*NUCB2*[c]	−1.24	0.20	.01
Protein FAM3D	*FAM3D*[c]	−1.22	−0.36	.009
Trypsin-1	*PRSS1*[c]	−1.64	−1.06	.02
6-Phosphogluconate dehydrogenase, decarboxylating	*PGD*[a]	−0.73	−1.4	<.001
Aldehyde dehydrogenase, dimeric NADP-preferring	*ALDH3*[a]	−0.99	−1.29	<.001
Antileukoproteinase	*SLPI*[a]	−2.21	−2.14	<.001
BPI fold−containing family A member 1	*BPIFA1*[a]	−2.39	−2.53	.02
BPI fold−containing family B member 1	*BPIFB1*[a]	−2.74	−2.67	.01
Cathepsin B	*CTSB*[a]	−0.92	−1.25	<.001
Cellular retinoic acid−binding protein 2	*CRABP2*[a]	−0.76	−1.38	.003
Chitotriosidase-1	*CHIT1*[a]	0.52	2.18	.03
Cornulin	*CRNN*[a]	−1.31	−1.56	.004
Coronin-1A	*CORO1A*[a]	−0.72	−1.24	.04
Desmocollin-2	*DSC2*[a]	−1.08	−1.22	.001
Glyceraldehyde-3-phosphate dehydrogenase	*GAPDH*[a]	−0.43	−1.36	.01
GTP-binding nuclear protein Ran	*RAN*[a]	−0.63	−1.34	.03
Immunoglobulin heavy constant gamma 2	*IGHG2*[a]	0.03	−1.38	.001
L-lactate dehydrogenase B chain	*LDHB*[a]	−0.85	−1.28	.014
Lipocalin-1	*LCN1*[a]	−2.94	−2.83	.01
Serpin B5	*SERPINB5*[a]	−0.92	−1.20	.02
Small proline-rich protein 3	*SPRR3*[a]	−2.19	−1.49	.04

Fold change threshold was ±1.2. Differential expression considered a false discovery rate of 0.05. Healthy individuals were considered as controls.
Ctrl, control; DE, differential expression; FC, fold change; OL, oral leukoplakia; PVL, proliferative verrucous leukoplakia.
[a] Proteins that only show the difference between proliferative verrucous leukoplakia and control groups.
[b] Proteins that show the difference between proliferative verrucous leukoplakia against oral leukoplakia and control groups at the same time.
[c] Proteins that only show the difference between proliferative verrucous leukoplakia and oral leukoplakia groups.

the dependent variable. The data were found to present a normal distribution and heteroscedastic based on asymmetry and kurtosis analysis, confirmed by Box's Test of Equality of Covariance Matrices and Levene's Test of Equality Variances (both $P < .001$). Therefore, Pillai's trace was used to evaluate the multivariate ANOVA of the 3 biomarkers, which revealed statistically significant differences across the groups for each biomarker ($P < .0001$).

Table 3
Differentially expressed proteins identified in the tissue that were simultaneously found in the saliva

Protein name	Gene symbol	Tissue			Saliva		
		FC PVL vs OL	FC PVL vs Ctrl	DE *q* value	FC PVL vs OL	FC PVL vs Ctrl	DE *q* value
40S ribosomal protein SA	*RPSA*	2.1	1.6	.000	−0.3	−0.7	.204
Histone H4	*HIST1H4A*	1.9	1.6	.024	1.2	1.0	.335
14-3-3 protein epsilon	*YWHAE*	1.7	2.1	.001	−0.2	−0.3	.433
Alpha-enolase	*ENO1*	1.6	1.4	.032	−0.5	−1.0	.010
14-3-3 protein beta/alpha	*YWHAB*	1.5	1.0	.007	0.1	−0.1	.986
Heat shock 70 kDa protein 1B	*HSPA1B*	1.4	1.3	.017	0.3	0.1	.445
Serpin B5	*SERPINB5*	1.4	1.4	.001	−0.9	−1.2	.013
Heat shock cognate 71 kDa protein	*HSPA8*	1.3	1.3	.026	−0.3	−0.3	.261
14-3-3 protein theta	*YWHAQ*	1.3	1.4	.024	−1.3	−2.1	.061
Fructose-bisphosphate aldolase A	*ALDOA*	1.3	0.9	.011	−0.5	−1.1	.004
Keratin, type II cytoskeletal 1	*KRT1*	1.1	1.5	.044	−1.1	−1.8	.041
Desmoglein-1	*DSG1*	1.1	1.6	.039	−1.0	−1.7	.002
Rab GDP dissociation inhibitor beta	*GDI2*	1.0	1.2	.000	−0.6	−0.9	.024
Glyceraldehyde-3-phosphate dehydrogenase	*GAPDH*	1.0	0.4	.014	−0.4	−1.4	.070
ATP synthase subunit beta, mitochondrial	*ATP5B*	0.9	1.1	.020	−1.2	−0.6	.106
Keratin, type I cytoskeletal 10	*KRT10*	0.8	1.4	.045	−1.1	−0.9	.028
14-3-3 protein zeta/delta	*YWHAZ*	0.5	0.9	.030	−0.5	−0.7	.079
Keratin, type I cytoskeletal 16	*KRT16*	0.3	2.2	.014	−0.7	−0.6	.088
Keratin, type I cytoskeletal 14	*KRT14*	0.1	1.2	.019	−1.3	−1.8	.030
Keratin, type II cytoskeletal 4	*KRT4*	−1.1	−1.9	.045	−0.5	−0.2	.351

Fold change threshold was ±1.2. Differential expression considered a false discovery rate of <0.05. Inflammatory fibrous hyperplasia (tissue) and healthy individuals (saliva) were considered as controls.
Ctrl, control; DE, differential expression; FC, fold change; OL: oral leukoplakia; PVL, proliferative verrucous leukoplakia.

The Games–Howell post hoc test was performed, demonstrating an increased intraepithelial expression of CALR in the PVL compared with OL (95% CI, −46.18 to −11.10; $P = .001$). Similarly, YWHAQ and RACK1 proteins showed a similar trend in the progression from normal to DPMOs. YWHAQ exhibited a reduced intraepithelial expression in IFH compared with OL (95% CI, −42.07 to −1.42; $P = .033$) and PVL (95% CI, −53.41 to −21.64; $P < .0001$), whereas RACK1 displayed the same expression pattern in IFH compared with OL (95% CI, −62.20 to −21.39; $P < .0001$) and PVL (95% CI, −62.60 to −30.06; $P < .0001$). Immunostaining quantification and statistical differences for CALR, YWHAQ, and RACK1 are presented in Figure 4. Additionally, we conducted a multivariate ANOVA with 2 independent factors: clinicopathological diagnosis and grade of oral epithelial dysplasia. No statistically significant differences were found when considering the binary system of oral epithelial dysplasia grading. However, we observed a significant difference in the intensity of CALR (95% CI, −56.79 to −7.85; $P < .001$) and RACK1 (95% CI, −22.76 to −26.18; $P < .002$) staining only in the OL group, when comparing samples without and with oral epithelial dysplasia (Fig. 5).

Discussion

MS-based proteomics has been proven to be a valuable approach for identifying differentially expressed proteins and posttranslational modifications in OPMD tissues. This technique provides insights into the molecular mechanisms underlying the disease and can contribute to the development of more effective treatments. Additionally, MS-based proteomics enables the identification of biomarkers for early diagnosis and monitoring of disease progression.[23,24]

In this study, we demonstrated the utility of performing a proteomic analysis of laser microdissected epithelial tissue to identify potential diagnostic and therapeutic targets of OPMDs, particularly PVL. This analysis confirmed overlapping protein expression between oral tissues and saliva samples, highlighting the higher protein content in PVL samples compared with OL and control samples. Significant differences in pathway analysis were also observed between PVL and OL, with the immune-related pathways being particularly prominent. This finding suggests that the immune system plays a crucial role in the immunosurveillance process,[25,26] and the higher number of altered pathways in PVL may contribute to the higher risk of malignant transformation compared with that in OL.[6]

Furthermore, this higher potential for malignancy could also be related to the higher number of altered cell cycle pathways detected in the PVL samples. Regardless, in response to cell cycle deregulation, cells may employ alternative mechanisms, as evidenced by the higher number of proteins associated with apoptosis and DNA repair pathways in PVL samples. This molecular pattern correlates with the clinical manifestation of PVL, which exhibits a slow and progressive malignant transformation over time[5,27] without sufficient strength for autoregulation, as 14.3% to 75% of these lesions progress to carcinoma.[6]

Qualitative and PCA of tissue and saliva samples demonstrated that it is possible to differentiate and cluster the studied groups based on their proteomes, suggesting distinct molecular compositions among lesions. IHC validation confirmed differential expression in the studied groups. However, only CALR showed a statistically significant difference between OL and PVL. Furthermore, when comparing samples with and without oral epithelial dysplasia, CARL and RACK1 levels were only altered in OL, suggesting that these proteins may not be associated with the grade of oral epithelial dysplasia in this OPMD. These findings suggest that the current grading system for epithelial dysplasia may have limited value in predicting the malignant transformation of PVL. This might be attributed to the nature of the disease because PVL lesions often do not reveal major cytologic changes, even when

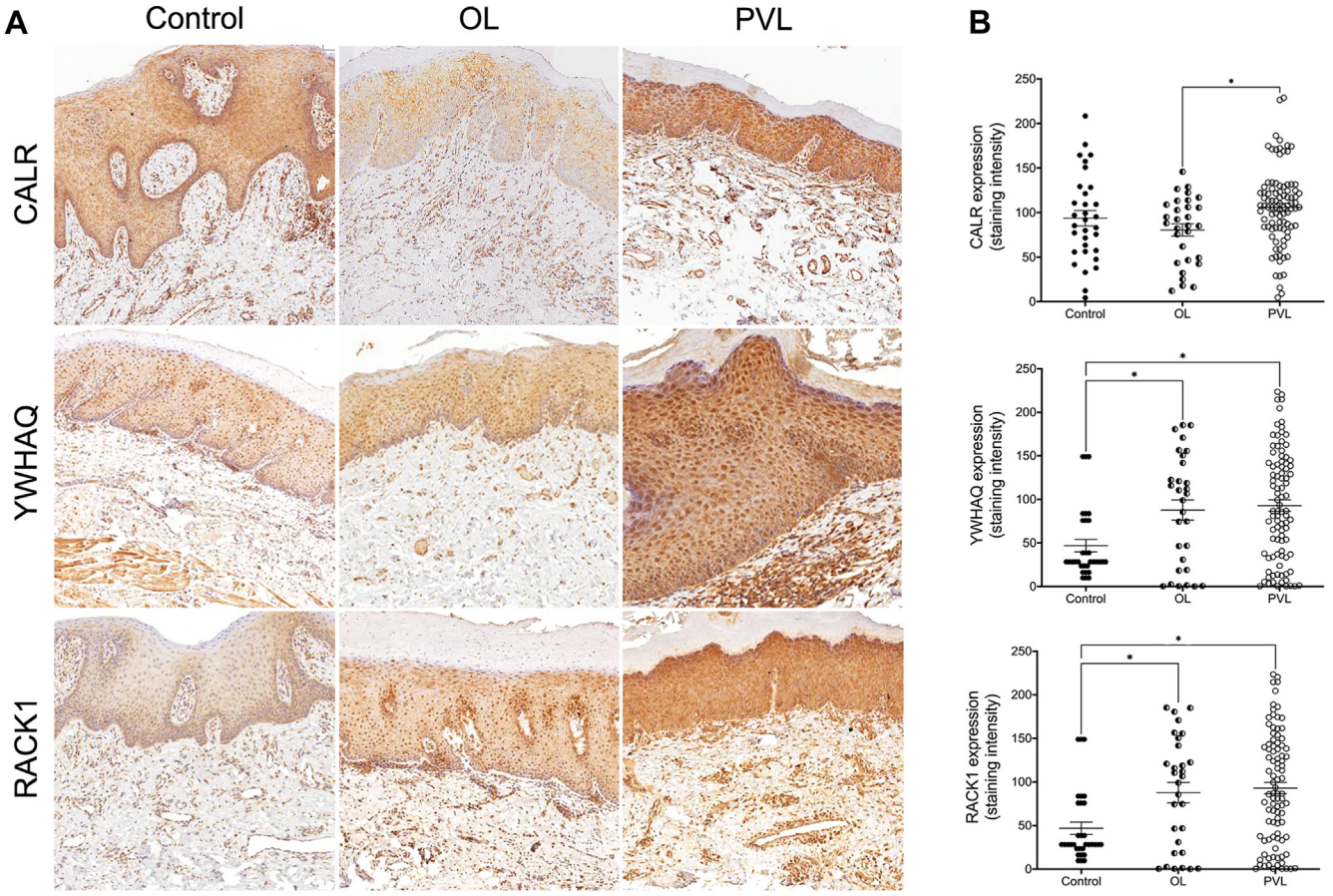

Figure 4.
Immunohistochemical staining for CALR, YWHAQ, and RACK1 expression in the proliferative verrucous leukoplakia (PVL), oral leukoplakia (OL), and inflammatory fibrous hyperplasia samples. (A) Representative photomicrographs demonstrating the immunostaining pattern of each marker in the respective groups (single stain, ×200). (B) Quantification and statistical analysis of staining intensity for CALR, YWHAQ, and RACK1 evaluated in the intraepithelial area for each group. *$P < .05$.

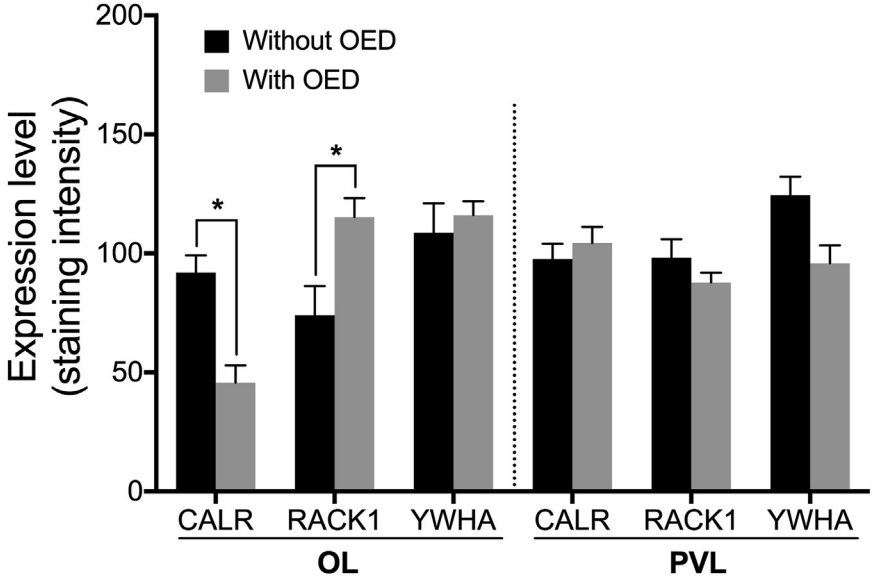

Figure 5.
Association of CALR, YWHAQ, and RACK1 expression with the presence and absence of tissue dysplasia in oral leukoplakia (OL) and proliferative verrucous leukoplakia (PVL) groups. Two-way analysis of variance revealed the statistical differences for CALR and RACK1 expression between samples without and with oral epithelial dysplasia in the OL group. OED, oral epithelial dysplasia. *$P < .05$.

there are significant architectural changes.[28] Visualizing the expression patterns of these 3 markers could help improve the interobserver and intraobserver variability that occurs among pathologists and dental surgeons when diagnosing OPMD based only on the clinical and histopathological criteria.[7-10,29] Furthermore, studying the proteome through differential expression of proteins could be useful for understanding the biological behavior in terms of malignant transformation, especially in PVL lesions.

The analysis of fold change values in tissue samples highlighted the YWHA protein family, indicating their importance in the context of PVL. Furthermore, the YWHA cluster was connected to the activity and function of the proteins composing the matrix of PVL samples. In addition, the network projected through STRING showed clustering of the same proteins, which have been implicated in the regulation of several intracellular signaling processes, including the cell cycle, cell proliferation, cell migration, DNA damage checkpoint, apoptosis, autophagy, modulation of gene expression, and regulation of oncoproteins and tumor suppressor proteins. The binding of YWHA proteins modulates their activity, cellular localization, stability, and interactions.[30,31] Moreover, YWHA overexpression is strongly associated with the development, poor survival rates, and poor treatment outcomes in brain, lung, breast, liver, and bladder tumors.[30,32-35] YWHAQ, a member of the YWHA protein family, was identified in both tissue and saliva samples. However, statistical significance was not reached in saliva samples, probably because of the limited number of samples included in the LC-MS/MS. The higher fold change of YWHAQ in tissue compared with OL may represent its involvement in various biological processes and pathways, whereas the lower expression in saliva could be attributed to the limited free/nonlinked form of YWHAQ. Nevertheless, the presence of YWHAQ in the PVL should be further investigated as it might contribute to higher fold change values observed in tissue samples. Furthermore, IHC analysis revealed higher YWHAQ expression in the OPMD samples than in that control group, supporting its potential role in the malignant transformation of OPMD. The absence of a statistical difference in the expression of YWHAQ between patients with OPMD can be attributed to the presence of this protein, along with other members of the YWHAQ family, potentially contributing to shared pathways in both OPMD lesions.

Overexpression of YWHAQ has been detected in various solid tumors with antiadhesive properties, promoting a positive effect on tumor cell adhesion and growth,[36] indirectly blocking cell apoptosis, and promoting tumor progression.[32,37] In addition, overexpression of YWHAQ has been correlated with advanced-stage, lymph node metastasis, estrogenic negative status, and poor clinical outcome.[30,38,39] In addition, the YWHA cluster observed in this study was linked to 2 clusters mainly composed of chaperone proteins, such as heat shock proteins, CALR, as well as others including ALDOA, GAPDH, GDI2, and RAB11A. Heat shock proteins maintain, stabilize, and activate oncogenic proteins.[40,41] In the present study, CALR was found exclusively in tissue samples, and its absence in saliva could be attributed to its presence between the endoplasmic reticulum and the extracellular surface of the plasma membrane. When produced extracellularly, CALR binds to other cell surfaces of the plasma membrane,[42] possibly acting as a protective factor against malignant transformations. Furthermore, IHC analysis revealed higher expression of CALR in PVL samples compared with the OL group, but it failed to distinguish between OPMD and the control group, possibly due to the inflammatory nature of IFH. CALR is highly related to carcinogenesis and acts as a cell surface marker for phagocytosis by macrophages or other immune cells such as dendritic cells.[43] Although increased CALR expression has been linked to increased tumor cell proliferation; cell growth; upregulation of vascular endothelial growth factor; and metastasis in some cancers, such as ovarian, pancreatic, gastric, prostate, and oral cancers, this relationship does not imply causation.[42,43] Moreover, contradictory evidence suggests that CALR has a negative effect on cancer cell survival and proliferation, and it is currently unknown whether CALR has a pro-oncogenic, antitumoral, or dual effect depending on its cellular location and protein status,[43,44] or whether its level, particularly in malignancies, is a cellular reaction to stop the malignancy process, acting simply as an antitumor protein.

The RACK1-linked cluster of ribosomal proteins plays a role in carcinogenesis through extraribosomal actions, including apoptosis, cell cycle arrest, cell proliferation, neoplastic transformation, cell migration, and invasion. Overexpression of ribosomal proteins has also been reported in various cancers, including prostate, gastric, lung, esophageal, and breast cancers, osteosarcoma, renal cell carcinoma, melanoma, glioblastoma, and ovarian tumors. Overexpression of RACK1 in OSCC was strongly associated with cell survival and correlated with the severity of epithelial dysplasia, clinical stage, lymph node involvement, recurrence, and aggressive behavior, all of which indicate a poor clinical outcome.[45,46] In the present study, RACK1 was only detected in tissue samples and was differentially expressed in PVL compared with OL and the control. RACK1 is a receptor protein found mainly in the cell nucleus, perinuclear area, and plasma membrane, and rarely in the extracellular medium, which could explain its absence in saliva.[47] Furthermore, IHC analysis revealed lower RACK1 expression in the control compared with the other 2 groups. As observed for YWHAQ, RACK1 appeared to effectively differentiate patients with OPMD from controls but did not differentiate OPMD subgroups. Perhaps, the higher expression of these 2 biomarkers serves as a common denominator in the malignant transformation process of OPMD.

Despite both PVL and OL being classified as OPMD, this study revealed that these lesions have a different protein profile. Consequently, it is imperative to consider them as 2 separate entities, especially due to their clinical behavior sustained by their protein machinery, which facilitates the malignant transformation processes in varying proportions depending on the lesion.

The main limitation of this research is the small sample size used in the proteomic analysis due to the nature of the MS assays. Also, low-expressed proteins could not be detected because they were overlapped by the highly expressed proteins. The DDA method used in the discovery process has low repeatability due to stochastic sampling, whereas the primary constraints of the proteomic approach based on SWATH-MS analysis are mostly limited by the constitution of the spectrum library. Future studies will greatly expand the spectrum library by combining additional discovery-based DDA analysis of mouth epithelial tissue and/or cell types associated with OL and PVL. Nevertheless, it should be noted that there is no need for further experiments to reacquire MS data because existing SWATH MS data sets may be retroactively examined with new spectrum libraries. Additionally, future proteomics assays could perform sampling arrangements by dysplasia degree before discovery analyses and then evaluate the intragroup and intergroup differential expressions.

In conclusion, the findings from this study suggest that YWHA, CALR, and RACK1 proteins may be involved in the malignancy of PVL and OL. Moreover, CALR and RACK1 may play distinct roles in the malignant transformation of PVL and OL. Further research is required to enhance our understanding of their roles in the malignancy process of PVL and to identify new targets for the development of diagnostic tools and

treatments, ultimately improving the prognosis of patients with PVL.

Author Contributions

E.A., M.P.S., P.G.V., J.D.A., I.L.F., and A.B. designed and supervised the study. M.P.C.V., J.M.S.P., A.B.C., M.G.V., P.G.V., A.G.G., J.D.A., M.R., T.S., J.R., E.P.I., M.G.O.A., T.M.F., and A.B. coordinated the acquisition, distribution, and quality evaluation of the tissue and saliva samples. S.B.B., C.M.P., M.G.V., G.C.V.C., F.C.S.N., J.A.M.E., D.A.P., E. P. I., I.L.F., and A. B. performed the analyses and quality control of the MS data. C.O.B., M.P.P., J.M.S.P., T.M.F., H.A.S., J.E.L., E.V.S., and M.R. performed immunohistochemical data analyses. E.A., S.B.B., C.M.P., M.G.V., G.C.V.C., F.C.S.N., J.A.M.E., D.A.P., E.P.I., and I.L.F. conducted proteomic data analyses. E.A. and A.B. wrote the manuscript. All authors have reviewed and approved the submission of this manuscript.

Data Availability

The raw data obtained from LC-MS/MS analysis in this study can be accessed through the ProteomeXchange Consortium via the PRIDE partner repository (http://www.ebi.ac.uk/pride). The data for saliva samples can be found under the identifier PXD039647, and the data for tissue samples can be found under the identifier PXD039947.

Funding

E.A. received funding for this research from the Estudantes-Convênio de Pós-Graduação (PEC-PG, 88881.154490/2017-01), Brazil. A.B. received funding for this research from the São Paulo Research Foundation (FAPESP, grant #2017/01438-0) and the National Council for Scientific and Technological Development (CNPq, grant #423945/2016-5). This study partly was supported by the Coordenação de Aperfeiçoamento de Pessoal de Nível Superior, Brazil (CAPES, Finance Code 001).

Declaration of Competing Interest

None reported.

Ethics Approval and Consent to Participate

This multicenter study, conducted in accordance with the Helsinki Declaration, was approved by the institutional ethics committees of the 2 participating centers (Brazil approval number CAAE 34361814.9.0000.5416 and Spain approval number 2019/271), and informed consent was obtained from all patients.

Supplementary Material

The online version contains supplementary material available at https://doi.org/10.1016/j.labinv.2023.100222

References

1. Warnakulasuriya S, Kujan O, Aguirre-Urizar JM, et al. Oral potentially malignant disorders: a consensus report from an international seminar on nomenclature and classification, convened by the WHO Collaborating Centre for Oral Cancer. *Oral Dis*. 2021;27(8):1862–1880. https://doi.org/10.1111/odi.13704
2. Ranganathan K, Kavitha L. Oral epithelial dysplasia: classifications and clinical relevance in risk assessment of oral potentially malignant disorders. *J Oral Maxillofac Pathol*. 2019;23(1):19–27. https://doi.org/10.4103/jomfp.JOMFP_13_19
3. Aguirre-Urizar JM, Lafuente-Ibáñez de Mendoza I, Warnakulasuriya S. Malignant transformation of oral leukoplakia: systematic review and meta-analysis of the last 5 years. *Oral Dis*. 2021;27(8):1881–1895. https://doi.org/10.1111/odi.13810
4. Villa A, Woo SB. Leukoplakia—a diagnostic and management algorithm. *J Oral Maxillofac Surg*. 2017;75(4):723–734. https://doi.org/10.1016/j.joms.2016.10.012
5. Torrejon-Moya A, Jané-Salas E, López-López J. Clinical manifestations of oral proliferative verrucous leukoplakia: a systematic review. *J Oral Pathol Med*. 2020;49(5):404–408. https://doi.org/10.1111/jop.12999
6. Iocca O, Sollecito TP, Alawi F, et al. Potentially malignant disorders of the oral cavity and oral dysplasia: a systematic review and meta-analysis of malignant transformation rate by subtype. *Head Neck*. 2020;42(3):539–555. https://doi.org/10.1002/hed.26006
7. Kujan O, Oliver RJ, Khattab A, Roberts SA, Thakker N, Sloan P. Evaluation of a new binary system of grading oral epithelial dysplasia for prediction of malignant transformation. *Oral Oncol*. 2006;42(10):987–993. https://doi.org/10.1016/j.oraloncology.2005.12.014
8. Fleskens SA, Bergshoeff VE, Voogd AC, et al. Interobserver variability of laryngeal mucosal premalignant lesions: a histopathological evaluation. *Mod Pathol*. 2011;24(7):892–898. https://doi.org/10.1038/modpathol.2011.50
9. Sperandio M, Brown AL, Lock C, et al. Predictive value of dysplasia grading and DNA ploidy in malignant transformation of oral potentially malignant disorders. *Cancer Prev Res (Phila)*. 2013;6(8):822–831. https://doi.org/10.1158/1940-6207.CAPR-13-0001
10. Upadhyaya JD, Fitzpatrick SG, Cohen DM, et al. Inter-observer variability in the diagnosis of proliferative verrucous leukoplakia: clinical implications for oral and maxillofacial surgeon understanding: a collaborative pilot study. *Head Neck Pathol*. 2020;14(1):156–165. https://doi.org/10.1007/s12105-019-01035-z
11. Capella DL, Gonçalves JM, Abrantes AAA, Grando LJ, Daniel FI. Proliferative verrucous leukoplakia: diagnosis, management and current advances. *Braz J Otorhinolaryngol*. 2017;83(5):585–593. https://doi.org/10.1016/j.bjorl.2016.12.005
12. Lorenzo-Pouso AI, Pérez-Sayáns M, Bravo SB, et al. Protein-based salivary profiles as novel biomarkers for oral diseases. *Dis Markers*. 2018;2018, 6141845. https://doi.org/10.1155/2018/6141845
13. Siravegna G, Marsoni S, Siena S, Bardelli A. Integrating liquid biopsies into the management of cancer. *Nat Rev Clin Oncol*. 2017;14(9):531–548. https://doi.org/10.1038/nrclinonc.2017.14
14. Johann DJ, Rodriguez-Canales J, Mukherjee S, et al. Approaching solid tumor heterogeneity on a cellular basis by tissue proteomics using laser capture microdissection and biological mass spectrometry. *J Proteome Res*. 2009;8(5):2310–2318. https://doi.org/10.1021/pr8009403
15. Tyanova S, Cox J. Perseus: A bioinformatics platform for integrative analysis of proteomics data in cancer research. In: von Stechow L, ed. *Cancer Systems Biology*. 1711. Springer; 2018:133–148. https://doi.org/10.1007/978-1-4939-7493-1_7
16. Fabregat A, Jupe S, Matthews L, et al. The reactome pathway Knowledgebase. *Nucleic Acids Res*. 2018;46(D1):D649–D655. https://doi.org/10.1093/nar/gkx1132
17. Muetze T, Goenawan IH, Wiencko HL, Bernal-Llinares M, Bryan K, Lynn DJ. Contextual hub analysis tool (CHAT): a cytoscape app for identifying contextually relevant hubs in biological networks. *F1000Res*. 2016;5:1745. https://doi.org/10.12688/f1000research.9118.2
18. Szklarczyk D, Santos A, von Mering C, Jensen LJ, Bork P, Kuhn M. STITCH 5: augmenting protein–chemical interaction networks with tissue and affinity data. *Nucleic Acids Res*. 2016;44(D1):D380–D384. https://doi.org/10.1093/nar/gkv1277
19. Carnielli CM, Macedo CCS, De Rossi T, et al. Combining discovery and targeted proteomics reveals a prognostic signature in oral cancer. *Nat Commun*. 2018;9(1):3598. https://doi.org/10.1038/s41467-018-05696-2
20. Tyanova S, Temu T, Sinitcyn P, et al. The Perseus computational platform for comprehensive analysis of (prote)omics data. *Nat Methods*. 2016;13(9):731–740. https://doi.org/10.1038/nmeth.3901
21. Pathan M, Keerthikumar S, Ang CS, et al. FunRich: an open access standalone functional enrichment and interaction network analysis tool. *Proteomics*. 2015;15(15):2597–2601. https://doi.org/10.1002/pmic.201400515
22. Pathan M, Keerthikumar S, Chisanga D, et al. A novel community driven software for functional enrichment analysis of extracellular vesicles data. *J Extracell Vesicles*. 2017;6(1), 1321455. https://doi.org/10.1080/20013078.2017.1321455
23. Farah CS, Fox SA. Dysplastic oral leukoplakia is molecularly distinct from leukoplakia without dysplasia. *Oral Dis*. 2019;25(7):1715–1723. https://doi.org/10.1111/odi.13156
24. Farah CS, Jessri M, Bennett NC, Dalley AJ, Shearston KD, Fox SA. Exome sequencing of oral leukoplakia and oral squamous cell carcinoma implicates

DNA damage repair gene defects in malignant transformation. *Oral Oncol*. 2019;96:42–50. https://doi.org/10.1016/j.oraloncology.2019.07.005
25. Zitvogel L, Tesniere A, Kroemer G. Cancer despite immunosurveillance: immunoselection and immunosubversion. *Nat Rev Immunol*. 2006;6(10):715–727. https://doi.org/10.1038/nri1936
26. Dunn GP, Old LJ, Schreiber RD. The immunobiology of cancer immunosurveillance and immunoediting. *Immunity*. 2004;21(2):137–148. https://doi.org/10.1016/j.immuni.2004.07.017
27. Reibel J, Gale N, Hille J, Hunt J, Lingen M, Muller S. Oral potentially malignant disorders and oral epithelial dysplasia. In: El-Naggar AK, Chan JK, Grandis JR, Takata T, Slootweg PJ, eds. *WHO Classification of Head and Neck Tumours*. 4th ed. International Agency for Research on Cancer; 2017:112–115.
28. Odell E, Kujan O, Warnakulasuriya S, Sloan P. Oral epithelial dysplasia: recognition, grading and clinical significance. *Oral Dis*. 2021;27(8):1947–1976. https://doi.org/10.1111/odi.13993
29. Warnakulasuriya S, Johnson NW, Van Der Waal I. Nomenclature and classification of potentially malignant disorders of the oral mucosa. *J Oral Pathol Med*. 2007;36(10):575–580. https://doi.org/10.1111/j.1600-0714.2007.00582.x
30. Khorrami A, Sharif Bagheri M, Tavallaei M, Gharechahi J. The functional significance of 14-3-3 proteins in cancer: focus on lung cancer. *Horm Mol Biol Clin Investig*. 2017;32(3), 20170032. https://doi.org/10.1515/hmbci-2017-0032
31. Tzivion G, Gupta VS, Kaplun L, Balan V. 14-3-3 proteins as potential oncogenes. *Semin Cancer Biol*. 2006;16(3):203–213. https://doi.org/10.1016/j.semcancer.2006.03.004
32. Yan Y, Xu Y, Gao YY, et al. Implication of 14-3-3ε and 14-3-3θ/τ in proteasome inhibition-induced apoptosis of glioma cells. *Cancer Sci*. 2013;104(1):55–61. https://doi.org/10.1111/cas.12033
33. Li N, Wang H, Fan J, et al. Overexpression of 14-3-3θ promotes tumor metastasis and indicates poor prognosis in breast carcinoma. *Oncotarget*. 2014;5(1):249–257. https://doi.org/10.18632/oncotarget.1502
34. Heidenblad M, Lindgren D, Jonson T, et al. Tiling resolution array CGH and high density expression profiling of urothelial carcinomas delineate genomic amplicons and candidate target genes specific for advanced tumors. *BMC Med Genomics*. 2008;1(1):3. https://doi.org/10.1186/1755-8794-1-3
35. Ko BS, Chang TC, Hsu C, et al. Overexpression of 14-3-3ε predicts tumour metastasis and poor survival in hepatocellular carcinoma. *Histopathology*. 2011;58(5):705–711. https://doi.org/10.1111/j.1365-2559.2011.03789.x
36. Martin D, Brown-Luedi M, Chiquet-Ehrismann R. Tenascin-C signaling through induction of 14-3-3 tau. *J Cell Biol*. 2003;160(2):171–175. https://doi.org/10.1083/jcb.200206109
37. Yun D, Wang H, Wang Y, et al. Shuttling SLC2A4RG is regulated by 14-3-3θ to modulate cell survival via caspase-3 and caspase-6 in human glioma. *EBioMedicine*. 2019;40:163–175. https://doi.org/10.1016/j.ebiom.2019.01.030
38. Hodgkinson VC, ELFadl D, Agarwal V, et al. Proteomic identification of predictive biomarkers of resistance to neoadjuvant chemotherapy in luminal breast cancer: a possible role for 14-3-3 theta/tau and tBID? *J Proteomics*. 2012;75(4):1276–1283. https://doi.org/10.1016/j.jprot.2011.11.005
39. Wang B, Liu K, Lin HY, Bellam N, Ling S, Lin WC. 14-3-3τ Regulates ubiquitin-independent proteasomal degradation of p21, a novel mechanism of p21 downregulation in breast cancer. *Mol Cell Biol*. 2010;30(6):1508–1527. https://doi.org/10.1128/MCB.01335-09
40. Zuehlke AD, Beebe K, Neckers L, Prince T. Regulation and function of the human HSP90AA1 gene. *Gene*. 2015;570(1):8–16. https://doi.org/10.1016/j.gene.2015.06.018
41. Calderwood SK, Gong J. Heat shock proteins promote cancer: it's a protection racket. *Trends Biochem Sci*. 2016;41(4):311–323. https://doi.org/10.1016/j.tibs.2016.01.003
42. Chiang WF, Hwang TZ, Hour TC, et al. Calreticulin, an endoplasmic reticulum-resident protein, is highly expressed and essential for cell proliferation and migration in oral squamous cell carcinoma. *Oral Oncol*. 2013;49(6):534–541. https://doi.org/10.1016/j.oraloncology.2013.01.003
43. Venkateswaran K, Verma A, Bhatt AN, et al. Emerging roles of calreticulin in cancer: implications for therapy. *Curr Protein Pept Sci*. 2018;19(4):344–357. https://doi.org/10.2174/1389203718666170111123253
44. Houen G. Commentary: Calreticulin-oncogene, anti-oncogene, or both? *Curr Protein Pept Sci*. 2019;20(1):111–112. https://doi.org/10.2174/1389203720011810311111149
45. Xu X, Xiong X, Sun Y. The role of ribosomal proteins in the regulation of cell proliferation, tumorigenesis, and genomic integrity. *Sci China Life Sci*. 2016;59(7):656–672. https://doi.org/10.1007/s11427-016-0018-0
46. Liu S, Liu J, Wang J, et al. RACK1 is an organ-specific prognostic predictor in OSCC. *Oral Oncol*. 2018;76:22–26. https://doi.org/10.1016/j.oraloncology.2017.10.025
47. Chuang NN, Huang CC. Interaction of integrin β1 with cytokeratin 1 in neuroblastoma NMB7 cells. *Biochem Soc Trans*. 2007;35(5):1292–1294. https://doi.org/10.1042/BST0351292